

Gluon number fluctuations with heavy quarks at HERA^{*}

ZHU Xiang-Rong(朱祥荣)^{1,2;1)} ZHOU Dai-Cui(周代翠)^{1,2;2)}

¹ Institute of Particle Physics, Huazhong Normal University, Wuhan 430079, China

² Key Laboratory of Quark & Lepton Physics, Huazhong Normal University, Ministry of Education, Wuhan 430079, China

Abstract: We study the effect of gluon number fluctuations (Pomeron loops) on the proton structure function at HERA. It is shown that the description of charm and bottom quarks and longitudinal structure functions are improved, with $\chi^2/\text{d.o.f}=0.803$ (fluctuations) as compared with $\chi^2/\text{d.o.f}=0.908$ (without fluctuations), once the gluon number fluctuations are included. We find that in the gluon number fluctuation case the heavy quarks do not play an important role in the proton structure function as the saturation model. The successful description of the HERA data indicates that the gluon number fluctuation could be one of the key mechanisms to describe the proton structure function at HERA energies.

Key words: deep inelastic scattering, gluon number fluctuations, proton structure function

PACS: 12.38.-t, 12.40.-y, 13.60.-r **DOI:** 10.1088/1674-1137/35/10/003

1 Introduction

For the last three decades, there has been tremendous progress in understanding the high-energy evolution in QCD. The first major description of the high-energy evolution is the Balitsky-Fadin-Kuraev-Lipatov (BFKL) [1] equation that was proposed in the leading logarithmic approximation. Further progress, a dipole picture, which was proposed by A. H. Mueller [2], is a factorization scheme for the scattering evolution in QCD at high-energy (at small- x). It allows one to describe the evolution of scattering amplitudes in hadronic interactions. In this picture, a gluon can be replaced by a quark-antiquark pair, a colorless dipole, and then the gluon-target scattering becomes a dipole-target scattering. If one takes into account the evolution of the dipole-proton scattering, then the scattering amplitude of the dipole-proton is given by Balitsky-JIMWLK [3, 4] equations in the limit where the number of colors N_c is large.

The Balitsky-Kovchegov (BK) equation [3, 5] is a non-linear evolution equation and does not include the effects of discreteness and, consequently, of the

fluctuations; it describes the scattering amplitude with rapidity $Y \equiv \ln 1/x$ of a dipole off a target (nucleus or hadron) at high energy in the mean-field approximation. There are two well known hallmarks of the BK equation, which are the geometric scaling behavior of the scattering amplitude and the energy dependence of the saturation scale. Tremendous theoretical progress has been achieved in recent years in the understanding of the QCD evolution at high energies beyond the mean-field approximation, e.g., beyond the BK equation. It has been understood how to include the discreteness and fluctuations of gluon numbers (Pomeron loops) in the evolution towards small Bjorken- x [6–9], both ignored in the Balitsky-JIMWLK equations and also in the BK equation. When taking into account the two elements, it leads to violation of the geometric scaling and to correction to the saturation scale, respectively; the evolution becomes a stochastic process and it needs to distinguish between the event-by-event amplitude $T(r, x)$, which corresponds to an individual gluon number realization of the evolved target dipole, and the physical amplitude $\langle T(r, Y) \rangle$, which is obtained by averaging

Received 10 December 2010, Revised 17 February 2011

^{*} Supported by NSFC (10875051, 11020101060), Programme of Science and Technology Department of Hubei Province (2009BFA010) and CCNU09C01002 (Key Grant)

1) E-mail: xgrgzhu@iopp.cnu.edu.cn

2) E-mail: dczhou@mail.cnu.edu.cn

©2011 Chinese Physical Society and the Institute of High Energy Physics of the Chinese Academy of Sciences and the Institute of Modern Physics of the Chinese Academy of Sciences and IOP Publishing Ltd

over all possible realizations of the target.

The charm and bottom structure functions were studied based on the saturation model used by Soyze in Ref. [10], who found that the value of the critical slope γ_c is a fundamental issue in the charm and bottom structure functions. It is shown that in the case of free γ_c the description of the HERA data is improved once the charm and bottom contributions to the proton structure function are included. It is known that the gluon number fluctuations on top of the saturation model can fit the proton structure function much better than the saturation model [11]. In this paper, we study the heavy quarks (charm and bottom) structure function by taking into account the gluon number fluctuation (Pomeron loop) effect beyond the saturation model. By comparing the outcomes which are obtained by fitting the experimental data with the IIM (Iancu, Itakura and Munier) and averaged IIM model [12], we conclude that the improvement of the description of the HERA data together with reasonable values of the parameters seems to indicate that the gluon number fluctuations could be one of the key mechanisms at HERA energies.

2 Mean-field approximation

In the mean-field approximation which assumes factorization: $\langle T^2 \rangle \approx \langle T \rangle \langle T \rangle$, the BK equation gives the rapidity Y -dependence of the T -matrix for a dipole of transverse size r scattering off a target,

$$\partial_Y T(Y, \rho) = \alpha_s \partial_\rho^2 T + \alpha_s T - \alpha_s T^2, \quad (1)$$

where $\rho = \ln 1/r^2 Q_s^2$. One of the main results following from the BK equation is the so-called geometric scaling behaviour of the scattering amplitude,

$$T(r, Y) = T(r^2 Q_s^2(Y)), \quad (2)$$

where $Q_s(Y)$ is the saturation momentum, which is a characteristic scale of the gluon distribution in the target. The T -matrix depends only on a single variable $r^2 Q_s^2(Y)$ instead of depending on r and Y separately, which seems well supported by HERA data [12, 13].

Another hallmark extracted from the BK equation is the rapidity dependence of the saturation scale, which separates the saturated ($r \gg 1/Q_s(Y)$) from the dilute ($r \ll 1/Q_s(Y)$) regime. It can be extracted from the BK equation [14–16]

$$Q_s^2(Y) = Q_0^2 \exp \left[\frac{2\alpha_s N_c}{\pi} \frac{\chi(\lambda_0)}{1-\lambda_0} Y \right], \quad (3)$$

where $\chi(\lambda) = 2\psi(1) - \psi(\lambda) - \psi(1-\lambda)$, with $\psi(\lambda) =$

$d \ln \Gamma(\gamma)/d\gamma$, is the eigenvalue of the Balitsky-Fadin-Kuraev-Lipatov kernel and $\lambda_0 = 0.372$.

To fit the HERA data by including the Pomeron loop effect and heavy quarks contribution, we use for the event-by-event amplitude the IIM model [12] which was obtained by solving the BK equation,

$$T^{\text{IIM}}(r, Y) = \begin{cases} T_0 \left(\frac{r Q_s(s)}{2} \right)^{2 \left(\lambda_s + \frac{\ln(2/r Q_s(s))}{\kappa \lambda Y} \right)}, & r Q_s(x) < 2 \\ 1 - \exp[-a \ln^2 b r Q_s(x)], & r Q_s(x) > 2. \end{cases} \quad (4)$$

It uses the saturation momentum the leading Y -dependence, $Q_s(x) = (x_0/x)^\lambda$, in the fit of the experimental data. The parameter λ controlling the energy dependence of the saturation scale and x_0 , being the value of x at $Q_s = 1$ GeV, are free parameters. The constant $\kappa = \chi''(\lambda_s)/\chi'(\lambda_s) \approx 9.9$ is a leading-order (LO) result achieved from the BK equation [14]. The factor T_0 in the first line of Eq. (4) is a constant around 0.5 for $r = 1/Q_s(Y)$. The coefficients a and b are obtained by the condition in Eq. (4) and its slope is continuous at $r Q_s = 2$.

The ‘‘BK-diffusion term’’ in the IIM-ansatz (4),

$$\left(\frac{r Q_s(s)}{2} \right)^{2 \frac{\ln(2/r Q_s(s))}{\kappa \lambda Y}} = \exp \left[- \frac{\ln^2(4/r^2 Q_s^2(s))}{2\kappa \lambda Y} \right], \quad (5)$$

explicitly violates the geometric scaling behavior. In order to get a better description of the deep inelastic scattering (DIS) data, this violation seems to be required. Without it, even allowing λ_s to be an additional fitting parameter, it cannot obtain an accurate description of the DIS data. For further details on the importance of the diffusion term, refer to Ref. [12].

3 Beyond the mean-field approximation

To go beyond the mean-field approximation one needs to take into account the effect of discreteness and fluctuations of gluon numbers. When including the fluctuations one has to distinguish between the even-by-event amplitude and the averaged (physical) amplitude. The physical amplitude, $\bar{T}(r, Y)$, is then given by averaging over all possible gluon number realizations/events, $\bar{T}(r, Y) = \langle T(r, Y) \rangle$, where $T(r, Y)$ is the amplitude for the dipole r scattering off a particular realization of the evolved proton at Y .

The fluctuations of the saturation momentum from event to event result from the dipole number

fluctuations in the low dipole occupancy region, with the dispersion increasing linearly with rapidity given by,

$$\sigma^2 = 2[\langle \rho_s^2 \rangle - \langle \rho_s \rangle^2] = DY, \quad (6)$$

where $\rho_s(Y) = \ln(Q_s^2(Y)/Q_0^2)$, D is the diffusion coefficient, whose value is known only for $\alpha \rightarrow 0$ (asymptotic energy) [6, 17]. Since the values of D and the exponent λ of the saturation scale, $Q_s^2(x) = 1 \text{ GeV}^2 (x_0/x)^\lambda$ are not known for finite energies, e.g., at HERA energy, in what follows we will treat them as free parameters, and the expectation value of the front position, $\langle \rho_s(Y) \rangle$, increases with rapidity as $\langle \rho_s(Y) \rangle = \ln(Q_s^2(Y)/Q_0^2)$ at high energy. The probability distribution of $\rho_s(Y)$ is approximately Gaussian [18, 19],

$$P(\rho_s) \approx \frac{1}{\sqrt{\pi\sigma^2}} \exp\left[-\frac{(\rho_s - \langle \rho_s \rangle)^2}{\sigma^2}\right]. \quad (7)$$

Based on the relation between high-energy QCD evolution and reaction-diffusion processes in statistical physics [20], the gluon number fluctuation effect is taken into account by averaging over all event-by-event amplitudes [21],

$$\begin{aligned} \langle T(\rho - \rho_s(Y)) \rangle &= \int d\rho_s T(\rho - \rho_s(Y)) P(\rho_s(Y)) \\ - \langle \rho_s(Y) \rangle &= \mathcal{T} \left(\frac{\rho_s(Y) - \langle \rho_s(Y) \rangle}{\sqrt{DY}} \right), \end{aligned} \quad (8)$$

where $T(\rho - \rho_s(Y))$ is the amplitude for the dipole scattering off a particular realization of the evolved proton at Y .

4 Numerical results

It is shown in Ref. [11] that the gluon number fluctuations improve the description of the HERA data with respect to the IIM model which only considers the parton saturation effect at high-energy QCD. The saturation exponent λ is equal to 0.252 and 0.192 of the IIM model and IIM with the Pomeron loop effects; the values of $\chi^2/\text{d.o.f}$ of the IIM model and IIM with the pomeron loop effects are 0.983 and 0.807, respectively. The improvement of $\chi^2/\text{d.o.f}$ indicates that the Pomeron loop effects possibly exit at HERA energies. In this section we will fit the HERA data by taking into account the Pomeron loop effects and the heavy quarks contribution to the proton structure functions.

In the DIS the projectile and the target interact by exchanging a virtual photon. The virtual photon fluctuates into a quark-antiquark pair of size r , which

then interacts with the proton. The proton still carries most of the total energy, while the virtual photon has just enough energy to dissociate long before scattering into a dipole, which then scatters off the gluon fields in the proton. The cross section of the virtual photon-proton can be written in a factorized form as the following:

$$\sigma_{T,L}^{Y^*P}(x, Q^2) = \int d^2r \int_0^1 dz |\psi_{T,L}(r, z, Q^2)|^2 \sigma_{\text{dip}}(x, r), \quad (9)$$

where $\sigma_{T,L}$, $\psi_{T,L}$ and σ_{dip} are the virtual photon-proton cross section, the light-cone wave functions for the photon splitting into a $q\bar{q}$ pair (the ‘‘dipole’’) and the dipole-proton cross section, and Q^2 and z are the virtuality, the longitudinal momentum fraction of the photon, respectively. The labels T and L refer to the transverse and longitudinal parts, respectively.

Our fit includes the HERA data from the ZEUS Collaborations for the F_2 structure function within the kinematical range $x \leq 0.01$ and $0.045 \text{ GeV}^2 < Q^2 < 50 \text{ GeV}^2$ (see also [12] for more discussions on the range). From Eq. (9), it can write the F_2 structure function via the below relation [22],

$$F_2(x, Q^2) = \frac{Q^q}{4\pi^2 \alpha_{\text{em}}} (\sigma_T^{Y^*P}(x, Q^2) + \sigma_L^{Y^*P}(x, Q^2)). \quad (10)$$

The limit of the range of x is to ensure the formula works well and the upper limit on Q^2 has been chosen large enough to include a large amount of ‘‘perturbative’’ data points, but low enough to justify the use of the BFKL dynamics, rather than the DGLAP evolution. In our fit we use the same photon wave functions as in Refs. [23, 24], which can be calculated by QED [25],

$$\begin{aligned} &|\psi_T^{(f)}(r, z, Q^2)|^2 \\ &= e_f^2 \frac{\alpha_e N_c}{2\pi^2} \{ [z^2 + (1-z)^2] \bar{Q}_f^2 K_1^2(r\bar{Q}_f^2 + m_f K_0^2(r\bar{Q}_f^2)), \\ &|\psi_L^{(f)}(r, z, Q^2)|^2 = e_f^2 \frac{\alpha_e N_c}{2\pi^2} 4Q^2 z^2 (1-z)^2 K_0^2(r\bar{Q}_f^2), \end{aligned} \quad (11)$$

where the e_f and m_f denote the charge and mass of the quark with flavor f and

$$\bar{Q}_f^2 = z(1-z)Q^2 + m_f^2, \quad (12)$$

and three light quarks (u, d, s) with equal mass, namely, $m_u = m_d = m_s = 140 \text{ MeV}$ and two heavy quarks (c, b) with mass, $m_c = 1.5 \text{ GeV}$ and $m_b = 4.5 \text{ GeV}$, respectively. To fit the experimental data, the Bjorken variable x should be modified by $x(1 + 4m_f^2/Q^2)$. Note that the charm and bottom structure functions are easy to obtain by extracting the contribution of the charm and bottom quarks to the

structure function in (9), (10) and (11). Since there is a mismatch between H1 and ZEUS with regard to the data normalization, we have taken into account only the ZEUS data, and also only ZEUS has data in the low Q^2 region, e.g., in the saturation region. In order to fix the parameters, we minimize $\chi^2 = \sum_i (\text{model}(i, p_1, \dots, p_n) - F_2(i))^2 / (\text{error}(i))^2$, where the sum goes over the data points, p_1, \dots, p_n denote the parameters to be found, $F_2(i)$ is the experimental result for the F_2 structure function, and $(\text{error}(i))^2$ is the error of F_2 , which is calculated by the sum of the systematic error squared and the statistical error squared.

In Eq. (9) the dipole-proton cross section,

$$\sigma_{\text{dip}} = 2\pi R_p^2 \langle T(r, x) \rangle, \quad (13)$$

where $2\pi R_p^2$ is the outcome of the integration over the impact parameter, and R_p is referred to as the radius of the proton and is to be taken as a free normalization parameter in our paper. We will use the IIM model for the event-by-event amplitude, $T(r, x)$, and the physical amplitude, $\langle T(r, x) \rangle$, is obtained according to the rules outlined in the previous section¹⁾. In order to see the effects of gluon number fluctuations, in σ_{dip} we will use the event-by-event amplitude and the physical amplitude. When including the heavy quarks contribution, in the case of $T(r, x)$ there are four free parameters which will be fixed by fitting the HERA data: R_p , x_0 and λ coming via the saturation momentum $Q_s^2(x) = 1 \text{ GeV}^2 (x_0/x)^\lambda$ and γ_c (“critical slope”) [10]. In the case of the averaged (physical) amplitude, $\langle T(r, x) \rangle$, there is another free parameter, the diffusion coefficient D .

The outcomes from fitting the ZEUS data including light and heavy quarks and the effect of gluon number fluctuations deserve further comment:

1) Both fits of the IIM model with and without fluctuations seem to improve with heavy quarks. However, the improvement is not great, as can be seen from the comparable χ^2 values for T^{IIM} and $\langle T^{\text{IIM}} \rangle$ in Table 1 below and Table II in Ref. [11]. Note that the values of χ^2 of the IIM model with gluon number fluctuations are quite similar before and after inclusion of heavy quarks. It seems that in the case of gluon number fluctuations the heavy quarks contribution does not play a role in the description of HERA-inclusive DIS data, as can be seen from the comparison $\chi^2/\text{d.o.f}$ of physical amplitude in Table II in Ref. [11] with $\chi^2/\text{d.o.f}$ of physical amplitude in Table 1.

2) The value of λ becomes smaller after including the heavy quarks and fluctuations, which is in agreement with theoretical expectations, as can be seen from the comparison of Eq. (3) with Eq. (6) in Ref. [11].

3) The value of the critical exponent γ_c , which is obtained from the fit of ZEUS data with heavy quarks, seems larger than the LO values used in literature. However, it is in agreement with that from the various renormalization-group-improved NLO BFKL kernels [27].

4) The value of the diffusion coefficient D is sizeable, and surprisingly coincides with the values which have been found numerically by solving the (1+1)-dimensional toy model [28] and the Pomeron loop equations [29] in the fixed coupling case.

5) The value of x_0 in the fluctuations case is smaller than the value in the saturation model, this is because the fluctuations are the next-to-leading order contribution which could make the saturation scale less than 1 GeV at HERA energies.

Table 1. The IIM model: The parameters of the event-by-event (2 line) and of the physical (3 line) amplitude after including the heavy quarks contribution.

model/parameters	χ^2	$\chi^2/\text{d.o.f}$	$x_0 (\times 10^{-4})$	λ	γ_c	R_p/fm	D
T^{IIM}	138.06	0.908	0.126	0.217	0.731	0.661	0
$\langle T^{\text{IIM}} \rangle$	121.28	0.803	0.0017	0.162	0.689	0.836	0.1105

The contribution of the charm and bottom quarks to (11) can be used directly to compute the charm and bottom structure functions. We compare the results of our parametrization with the HERA measurements [30] of the charm and bottom structure functions. The parameterized structure functions are

naturally obtained from our formalism by only taking the charm or bottom contribution to the photon-proton cross-section in (9). The results from our model are plotted in Fig. 1 for charm and bottom structure functions, respectively. In both cases, we observe good agreement with the data. Similarly,

1) Note that in our fit we assume that the ansätze for $T(r, x)$, which are derived/motivated based on perturbative QCD, also work in low virtuality region, $Q^2 \leq 1 \text{ GeV}^2$. In this region non-perturbative physics [26] is involved which is only approximately given by our ansätze.

by taking the contribution only from the longitudinal part of the wave function in (9), we can obtain the longitudinal structure function. The parameterized longitudinal structure functions are shown in Fig. 2 together with the H1 measurements [31]. Again, the present parametrization gives a good description of the data. Together with the outcomes of Ref. [11], we can conclude that the gluon number fluctuations are a key mechanism for describing the HERA data. Finally, we note that in our fit we use only the ZEUS data to obtain the parameters, then we use these parameters to describe both the ZEUS and H1 heavy quarks structure functions and longitudinal structure functions.

5 Summary and discussion

In this paper, we have shown that the descriptions of the heavy quark structure function and longitudinal structure function are improved once the gluon number fluctuation effect and the heavy quarks contribution to the proton structure function are taken into account. The reasonable values of parameters, like the saturation exponent $\lambda = 0.162$, the diffusion coefficient $D = 0.1105$ seem to indicate that the gluon number could be one of the key mechanisms for describing the HERA data.

The gluon number fluctuations would become more clear at even higher collision energies as compa-

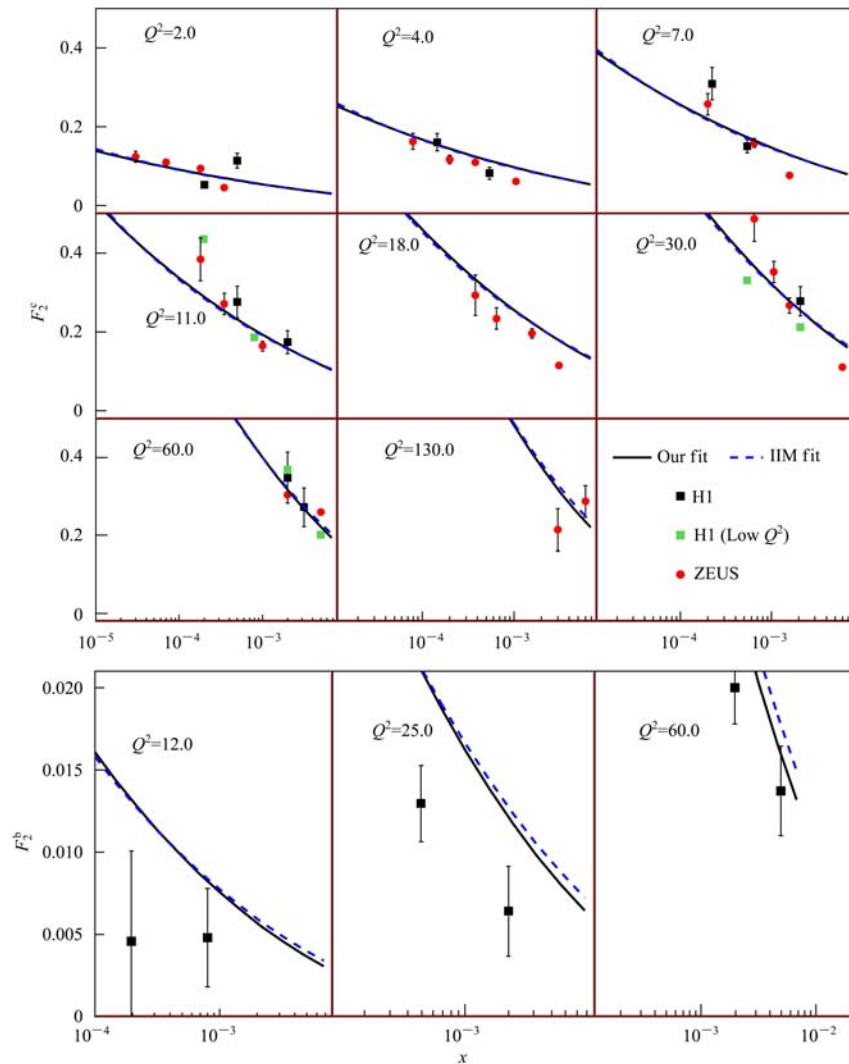


Fig. 1. The structure function versus x at different values of Q^2 . The up and down planes are charm and bottom structure functions, respectively. The solid lines represent the results of averaged IIM fitting experimental data and the dashed lines represent the results of IIM model fitting experimental data.

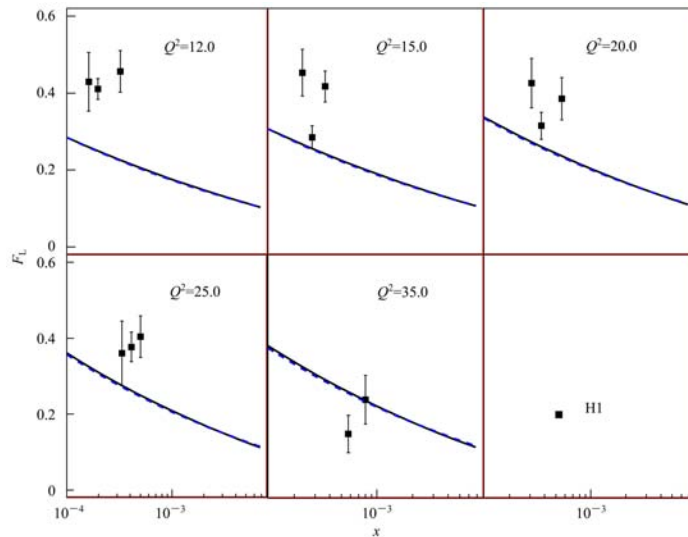


Fig. 2. The results of our fit for the longitudinal structure functions. The solid lines represent the results of averaged IIM fitting data and the dashed lines represent the results of IIM model fitting experimental data.

red with HERA energies. With increasing Y , according to the BK equation, the window for the geometric scaling behavior would increase, and the scaling violating term would become less important. On the other hand, the small- x dynamics including gluon

number fluctuations leads to a clearer diffusive scaling behavior with increasing Y [32]. The forthcoming LHC may tell us more whether geometric or diffusive scaling is more appropriate for the description of the observations in the LHC energy range.

References

- 1 Kuraev E A, Lipatov L N, Fadin V S. Sov. Phys. JETP, 1977, **45**: 199–204; Balitsky I I, Lipatov L N. Sov. J. Nucl. Phys., 1978, **28**: 822–829
- 2 Mueller A H. Nucl. Phys. B, 1994, **415**: 373–385; Mueller A H, Patel B. Nucl. Phys. B, 1994, **425**: 471–488; Mueller A H. Nucl. Phys. B, 1995, **437**: 107–126
- 3 Balitsky I I. Nucl. Phys. B, 1996, **463**: 99–157
- 4 Jamal J M, Kovner A, Leonidov A, Weigert H. Nucl. Phys. B, 1997, **504**: 415–431; Iancu E, Leonidov A, McLerran L. Nucl. Phys. A, 2001, **692**: 583–645; Weigert H. Nucl. Phys. A, 2002, **703**: 823–860
- 5 Kovchegov Y V. Phys. Rev. D, 1999, **60**: 034008
- 6 Mueller A H, Shoshi A I. Nucl. Phys. B, 2004, **692**: 175–208
- 7 Iancu E, Mueller A H, Munier S. Phys. Lett. B, 2005, **606**: 342–350
- 8 Mueller A H, Shoshi A I, Wong S M H. Nucl. Phys. B, 2005, **715**: 440–460; Iancu E, Triantafyllopoulos D N. Nucl. Phys. A, 2005, **756**: 419–467; Phys. Lett. B, 2005, **610**: 253–261; Kovner A, Lublinsky M. Phys. Rev. D, 2005, **71**: 085004
- 9 XIANG Wen-Chang. Nucl. Phys. A, 2009, **820**: 303c–306c
- 10 Soyez G. Phys. Lett. B, 2007, **655**: 32–38
- 11 Kozlov M, Shoshi A I, XIANG Wen-Chang. JHEP, 2007, **10**: 020
- 12 Iancu E, Itakura K, Munier S. Phys. Lett. B, 2004, **590**: 199–208
- 13 Stařto A M, Golec-Biernat K J, Kwiecinski J. Phys. Rev. Lett., 2001, **86**: 596–599
- 14 Iancu E, Itakura K, McLerran L. Nucl. Phys. A, 2002, **708**: 327–352
- 15 Gribov L V, Levin E M, Ryskin M G. Phys. Rept., 1983, **100**: 1–150
- 16 Mueller A H, Triantafyllopoulos D N. Nucl. Phys. B, 2002, **640**: 331–350
- 17 Brunet E, Derrida B, Mueller A H, Munier S. Phys. Rev. E, 2006, **73**: 056126
- 18 Marquet C, Soyez G, XIAO Bo-Wen. Phys. Lett. B, 2006, **639**: 635–641
- 19 XIANG Wen-Chang. Phys. Rev. D, 2010, **81**: 094004
- 20 Iancu E, Itakura K, Munier S. Phys. Lett. B, 2005, **606**: 342–350
- 21 XIANG Wen-Chang, WANG Sheng-Qin, ZHOU Dai-Cui. Chin. Phys. Lett., 2010, **27**: 072502
- 22 XIANG Wen-Chang, ZHOU Dai-Cui, WAN Ren-Zhuo, YUAN Xian-Bao. Chin. Phys. C (HEP & NP), 2009, **33**(02): 98–102
- 23 Golec-Biernat K J, Wüsthoff M. Phys. Rev. D, 1998, **59**: 014017
- 24 XIANG Wen-Chang. Eur. Phys. J. A, 2010, **46**: 91–98
- 25 Gieseke S, QIAO Cong-Feng. Phys. Rev. D, 2000, **61**: 074028
- 26 Ewerz C, Nachtmann O. Annals Phys., 2007, **322**: 1670–1726
- 27 Salam G P. JHEP, 1998, **07**: 019; Ciafaloni M, Colferai D, Salam G P. Phys. Rev. D, 1999, **60**: 114036
- 28 Iancu E, Santana Amaral J T, Soyez G, Triantafyllopoulos D N. Nucl. Phys. A, 2007, **786**: 131–163
- 29 Soyez G. Phys. Rev. D, 2005, **72**: 016007
- 30 Adloff C et al. (H1 collaboration). Phys. Lett. B, 2002, **528**: 199–214; Aktas A et al. (H1 collaboration). Eur. Phys. J. C, 2006, **45**: 23; Chekanov S et al. (ZEUS collaboration). Phys. Rev. D, 2004, **69**: 012004
- 31 Adloff C et al. (H1 collaboration). Eur. Phys. J. C, 2001, **21**: 33; Breitweg J et al. (ZEUS collaboration). Phys. Lett. B, 2000, **487**: 53–73; Chekanov S et al. (ZEUS collaboration). Eur. Phys. J. C, 2001, **21**: 443
- 32 XIANG Wen-Chang. Phys. Rev. D, 2009, **79**: 014012